Acta Cryst. (1959). **12**, 515

The Crystal Structure of Proto-enstatite, $MgSiO_3$*

By J. V. Smith

Department of Mineralogy and Petrology, Division of Earth Sciences, The Pennsylvania State University, University Park, Pennsylvania, U.S.A.

(*Received* 5 *November* 1958)

Proto-enstatite, at room temperature, is orthorhombic with 8 units of $MgSiO_3$ in a cell of dimensions $a = 9{\cdot}25$, $b = 8{\cdot}74$, $c = 5{\cdot}32$ Å, pseudo space group *Pbcn*. The atomic coordinates of the pseudo space group were determined from X-ray powder data. The SiO_3 chain is fully extended. One of the Mg atoms has an irregular coordination, which may be the reason for the instability of proto-enstatite at low temperature. The structure is very similar to that predicted by Atlas (1952).

Proto-enstatite is one of the five forms of $MgSiO_3$ that have so far been described (see Atlas, 1952 for literature survey). Only three of the five have been thought to have a field of stability—rhombic enstatite, clino-enstatite and proto-enstatite. Determination of the phase relations is difficult because of the sluggishness of the transformations between rhombic enstatite and the other two forms, and because of the ease of the inversion between the proto- and clino-forms. Whether clino- or proto-enstatite is the stable form at high temperature or whether both have a field of stability is still open to doubt, (Atlas, 1952; Foster, 1951; Boyd & Schairer, 1957), but it is certain that rhombic enstatite is the form stable at low temperatures and that proto-enstatite is unstable at the temperature of this structure determination. Proto-enstatite changes into clino-enstatite upon heating at 1400 °C., upon long standing at room temperature, and upon grinding. Thus the structure of the two forms must be related and, indeed, Atlas has used this as a basis for predicting a crystal structure for proto-enstatite.

This investigation has three objectives: establishing reliable crystallographic data for proto-enstatite, providing information on the atomic movements that occur during the phase transformations of $MgSiO_3$ and looking for a structural reason why stress can markedly effect the transformation for proto- to clino-enstatite. In this paper the first objective will be described: the second and third will be discussed later in collaboration with Dr N. Morimoto, who is currently engaged on a refinement of the structure of clino-enstatite.

The author is indebted to Dr F. R. Boyd of the Geophysical Laboratory, Washington, D.C. for attempting to grow large crystals of proto-enstatite. In spite of considerable labour, all attempts were unsuccessful and the structure determination has had, perforce, to be carried out on a powder sample. The conditions of crystallization were: treatment of an $MgSiO_3$ glass in a hydrothermal bomb at 1080 °C. for four days at 500 bars H_2O.

Crystallographic data

The X-ray powder diffraction pattern (Table 1) was indexed on an orthorhombic cell with

$$a = 9{\cdot}25,\ b = 8{\cdot}74,\ c = 5{\cdot}32\ \text{Å}\ (\pm 0{\cdot}005)\,.$$

Atlas obtained values of 9·25, 8·92, 5·25 Å for a specimen inverted from an iron- and aluminium-bearing anthophyllite. All reflections but one, (210), would obey the rules for the space group *Pbcn*, although little reliance could be placed on this pseudo space group because of the low number of unequivocally indexed reflections in the principal zones. The axes x and y should be interchanged to conform to common usage: however, the above order of axes is given to show the relation to clino-enstatite whose 8·8 Å axis is the symmetry axis. The volume of the unit cell is 430 Å^3 and the calculated specific gravity for 8 units of $MgSiO_3$ is 3·10.

Intensity data were obtained from powdered crystals smeared on a glass slide that was mounted on a diffractometer. Cu $K\alpha$ radiation and a proportional counter were used. The counter was moved at a rate of 0·1° 2θ per minute and the total number of counts printed out ten times per minute. A profile of each peak was plotted and the integrated intensity obtained. At low angles no difficulty was experienced in estimating the background level, but at angles greater than 2θ 30° the background was irregular, possibly because of the presence of peaks too small for recognition but sufficiently large for an upset of the background level. Above 2θ 70° the reflections were so irregular and difficult to index that no measurements were made. Divergence slits of 4° were used so that all the specimen was irradiated at all angles, permitting a simple correction for the Lorentz-polarization factor.

Measurements of lattice spacings and peak intensities (Table 1) for the X-ray Powder Data File were

---

* Contribution No. 58-15, College of Mineral Industries.

Table 1. *Powder data*

Values of I are the peak intensities measured with a Geiger counter diffractometer with specimen fully irradiated at all angles. pF^2 values were determined from the integrated intensities given by a proportional counter, after correction for the Lp factor. 1, 2, 3: three principal lines in order of peak intensity. Resolution of doublet begins at 32 degrees.

d obs.	I	hkl	2θ obs.	2θ calc.	pF^2 obs.	pF^2 calc.
		100		9·09		
		010		10·12		
6·35	2	110	13·94	13·94	50	72
		001		16·67		
4·62	1	200	19·20	19·19	40	72
		101		19·26		
		011		19·54		
4·372	3	020	20·31	20·32	210	216
4·086	1	210	21·75	21·74	140	
		111		21·80		26
		120		22·50		
		201		25·53		
		021		26·40		31
3·240	20	211	27·53	27·52	1280	830
		220	28·14	28·09	6260	740
3·171	100^1	121		28·14		4160
		300		28·96		
		030		30·69		
2·908	40^2	310	30·75	30·75	2370	2300
2·7792	3	130	32·18	32·21	190	270
2·7256	20	221	32·83	32·82	1400	1950
		301		33·57		
		002		33·69		16
		102	35·15	35·09	2670	1630
2·5509	30^3	031		35·09		
		311		35·15		830
		012		35·24		
		320		35·61		
		230		36·42		
2·4615	7	131	36·47	36·46	810	1230
		112		36·61		
		400		38·92		20
2·3046	20	202	39·05	39·05	1340	2580
		321		39·55		128
		022		39·65		20
2·236	5	231	40·30	40·29	460	800
		410		40·31		
2·229	2	212	40·43	40·44		141
		122		40·88		216
		040		41·28		8
		140		42·47		
		401		42·60		
2·1171	4	330	42·67	42·66	530	620
2·0610	2	411	43·89	43·90	340	1190
		420		44·28		28
		222		44·40		160
		041		44·81		135
		302		44·99		41
		240	45·92	45·89	4500	184
1·9746	20	141		45·92		2260
1·9681	20	331	46·08	46·10		1900
		032		46·19		
		312		46·23		512
		132		47·28		106
1·9075	1	421	47·63	47·63	310	540
1·8503	1	241	49·20	49·15	110	510
		500		49·21		
1·8287	1	322	49·82	49·83	270	392
		430		50·34		
1·8097	5	510	50·38	50·38	500	830
		242		50·45		116
		340		51·20		
		003		51·53		
		050		52·29		
		501		52·32		
1·7446	1	402	52·40	52·40	240	900
		103		52·53		
		013		52·65		
		150	53·35	53·29	4180	850
1·7157	12	431		53·40		970
		511		53·44		16
1·711	3	412	53·5	53·52		8
		113		53·65		415
		520		53·77		
		341		54·22		92
1·6598	3	042	54·30	54·30	750	680
1·6606	4	142	55·27	55·27	1240	968
		051		55·27		
		332		55·43		270
		203		55·48		
1·6420	20	023	55·95	55·93	5530	3050
		250		56·21		
		151		56·23		32
		213		56·55		32
		521		56·69		5
1·6205	4	422	56·76	56·77	2020	1190
		123		56·90		155
1·5880	1	440	58·03	58·02	840	340
		242		58·12		90
1·5635	1	251	59·03	59·05	550	565
		530		59·11		92
		223		59·70		
1·5428	1	600	59·95	59·96	730	900
		303		60·18		
		441		60·82		72
1·5210	1	350	60·85	60·87	670	450
		502		60·97		
		610		60·98		
		033		61·16		
		313		61·20		288
1·4988	15	531	61·85	61·87	7550	3810
		432		61·94		169
		512	62·02	61·98		1660
1·4951	15	133		62·06		2420
		601		62·70		
		342		62·70		0
		351		63·58		415
		052		63·66		
		611		63·70		270
1·4570	7	060	63·83	63·84	2180	1900
		620		63·99		16
		323		64·20		16
		160		64·72		
		233		64·73		32
		522		64·96		736
		540		66·13		
		403		66·41		
1·4029	1	061	66·60	66·64	590	164
		621		66·64		438
		450		67·06		
		260		67·33		8
		161		67·36		348
		413		67·37		46
1·3764	7	043	68·06	68·06	1700	1290
		541		68·73		3
		442		68·80		46
		630		68·85		
		143		68·91		92
1·3590	5	333	69·05	69·04	1680	5080

made with a Geiger-counter diffractometer using the same geometry as for the collection of integrated intensities. To calibrate the diffractometer, a separate smear mount of pure silicon of similar thickness to that of proto-enstatite was used, and the cell dimension a 5·4306 Å was assumed for the silicon. Tests have shown that this calibration method, if carefully applied, results in errors not greater than 0·02° in 2θ. The three strongest peaks of clino-enstatite were observed, indicating a proportion of about 5–10%. The I and pF^2 values in Table 1 differ for several reasons: rounding-off of the I values, Lorentz-polarization factor, peak *versus* integrated character, and random error.

Structure determination

It was obvious that when only one reflection did not obey the indicated pseudo space group, it would be necessary to ignore it and develop the average structure for the pseudo space group. Furthermore some simplifying assumptions had to be made in the adjustment of the atomic coordinates, for the customary process of automatic refinement by F-series was not possible. In many respects the structure determination was analogous to those carried out in the early nineteen-thirties.

The first simplifying assumption arose from a comparison of the repeat unit c with that for a chain of silicon–oxygen tetrahedra. By analogy with the other forms of $MgSiO_3$ it was obvious that an $(SiO_3)_\infty$ chain of the pyroxene type lay along the c-axis. Fortunately, it was possible to deduce that the chain in proto-enstatite was fully extended, for the length 5·32 Å, is actually slightly greater than that to be expected for a fully extended chain with the usual Si–O distances. For a regular tetrahedron the Si–O distance that corresponds to the 5·32 Å chain repeat is 1·63 Å, somewhat larger than the value of 1·60 Å, found in framework structures (Smith, 1954). Probably the tetrahedron is slightly distorted because of the unsymmetrical coordination.

The second simplifying assumption concerned the shape of the tetrahedron. As adjustment of the atomic coordinates, based on structure factor calculation, could not be expected to go beyond 0·1 Å, more accurate coordinates could be obtained by assuming a regular shape for the silicon–oxygen tetrahedra and using the standard distances which would be expected to be accurate to 0·03 Å. From this and the first assumption, the position of the chain could be specified by only three coordinates, if the space group were *Pbcn*. As the Mg atoms could either lie in one 8-fold position with three parameters or two 4-fold positions with one parameter each, this left only five or six variable parameters.

A few trials using *Pbcn* soon gave the coordinates for proto-enstatite (Table 2). Adjustment of the coordinates was as follows: the x and y coordinates were adjusted by use of the $hk0$ reflections. Four parameters are involved: the y coordinates of the two Mg atoms, and the two coordinates which specify the position of the chain. The position of the Mg_1 atom is crucial to the discussion of the stability of the structure, so the effect of varying its position is shown in Table 2. Change of the y-coordinate from 0·265 to 0·29 has a marked effect on the agreement between the calculated and observed structure factors and it seems safe to say that the y-coordinate is less than 0·29. The only remaining coordinate that required adjustment is the z-coordinate of the chain. Significant discrepancies developed when the z-coordinate was changed from 0·07 to 0·05 or 0·09 and these are regarded as the limits of error.

Table 2. *Effect on structure factors of the* Mg_1 *atom*

	$y = 0{\cdot}265$			$y = 0{\cdot}29$		
$hk0$	F_c	F_o	Δ	F_c	F_o	Δ
110	2·1	2·0	0·1	1·3	1·9	0·6
200	−3·0	2·6	0·4	−3·0	2·4	0·6
020	5·2	5·1	0·1	5·6	4·9	0·7
310	12·0	13·3	1·3	11·3	12·6	1·3
130	−4·1	3·8	0·3	−2·4	3·6	1·2
330	6·2	≤6·3	—	7·8	≤6·0	—
240	3·4	≤6·5	—	2·0	≤6·2	—
510	−7·2	6·1	0·9	−7·8	5·8	2·0
440	−4·6	6·4	1·8	−5·9	6·1	0·2
600	10·6	8·6	2·0	10·6	8·2	2·4
350	−5·3	≤6·0	—	−7·0	≤5·7	—
060	−15·4	16·2	0·8	−13·0	15·4	2·4
			7·7			11·4
		$R = 0{\cdot}12$			$R = 0{\cdot}19$	

The F_o values differ slightly because a different scaling factor has been used to make $\Sigma F_c = \Sigma F_o$.

Assessment of the accuracy of the coordinates is not easy. The value of $\Sigma(F_o^2 - F_c^2)/\Sigma F_o^2$ is 0·36 corresponding to an R-value of about 0·2. This is quite satisfactory for a structure with pseudo-symmetry but provides little basis for assessing accuracy. It is thought that the distances Mg–O and O–O are probably accurate to 0·1 Å and unlikely to be wrong by more than 0·2 Å.

Discussion

The structure displayed in Figs. 1, 2 and 3 is almost identical with that proposed but not proved by Atlas, testifying to the excellent use made by him of qualitative considerations. Only in one respect is his description of the structure in error: his structure like the one described here has symmetry *Pbcn* not the *Pbc*2 listed in his paper.

Possibly the most informative diagram is Fig. 3 where the familiar trapezium-shaped cross-sections of the pyroxene chain are visible in the xy projection. Each Mg atom lies in a polyhedron of six oxygen atoms arising from four different chains. In Fig. 1 the chains are seen lengthways on in the familiar position with the vertices pointing upwards (or downwards). The packing of the oxygen atoms shows up

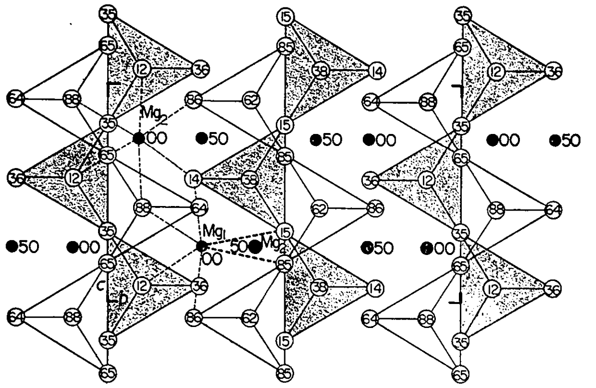

Fig. 1. *a*-axis projection: open circles, oxygen atoms; solid circles, magnesium atoms; silicon atoms omitted. Half of the $(SiO_3)_\infty$ chains are stippled. The two longer distances in the Mg_1–O polyhedron are shown by heavy dashed lines: all other Mg–O bonds by light dashed lines. The numbers give the *x* parameters in hundredths.

very neatly in this projection. The oxygen atoms lie closely on four levels $z \simeq 0{\cdot}15$, 0·35, 0·65, and 0·85, such that each level contains the 'basal' oxygen atoms of one chain and the 'vertical' oxygen atoms of another chain. The Mg atoms lie at 0·00 and 0·50 in octahedra, three of whose oxygen atoms come from one layer and three from another layer. For the Mg_2 atom the oxygen atoms fall closely at the corners of an octahedron, but for the Mg_1 atom the arrangement is quite distorted. The third projection (Fig. 2) gives another view of the length of the chain. The symmetrical arrangement of the chains is especially well displayed in this projection, as is the way in which the coordination of the Mg_2 atom depends on the stagger between the chains in the upper and lower halves of the unit cell.

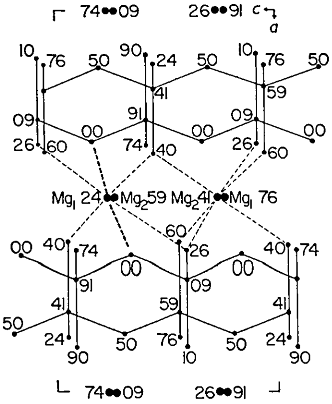

Fig. 2. *b*-axis projection: small solid circles, oxygen and silicon atoms; large solid circles, magnesium atoms. For clarity, the adjacent $(SiO_3)_\infty$ chains and the adjacent Mg atoms have been moved slightly apart. The two longer distances in the Mg_1–O polyhedron are shown by heavy dashed lines, all other Mg–O bonds by light dashed lines. The corners of the unit cell are shown, and the *y*-coordinates in hundredths of the cell edge.

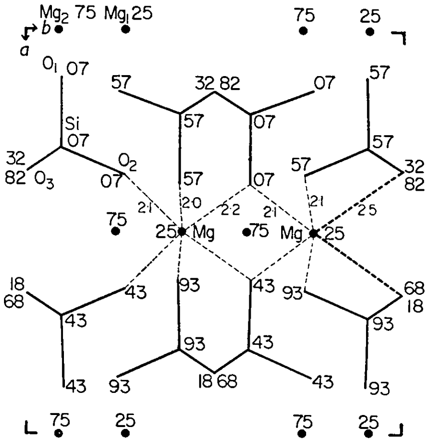

Fig. 3. *c*-axis projection. The silicon and oxygen atoms lie at the ends and intersections of the heavy lines, which act as skeletons for the familiar trapesium-shaped cross-sections of pyroxene chains. In the upper left one set of Si and O atoms are labelled. Magnesium atoms are shown by solid circles and the bonds to oxygen atoms by broken lines. The Mg–O distances are given in Å, the longer ones being emphasized by the heavier broken lines. The *z*-coordinates of all the atoms are shown, and the corners of the unit cell depicted.

Probably the most interesting aspect of the structure is the coordination of the Mg atoms. That of the Mg_2 atom is almost perfectly octahedral with distances Mg–O two each of 2·0, 2·1, 2·2 Å, in agreement with the standard value. That of the Mg_1 atom is quite different and is thought to be the weak spot, the Achilles heel, of the structure. The nature of the coordination is most easily seen from Fig. 1. The Mg_1 atom at height 0·00 lies below three oxygen atoms at a height of 0·14 of thereabouts and above three atoms at a height of 0·86 or thereabouts. For regular octahedral coordination the oxygen atoms would have to lie alternately up and down as a circuit of the Mg atom were made, a condition not obeyed by the Mg_1 atom. Four of the Mg_1–O distances are 2·1 Å, in agreement with the expected value for an Mg octahedron, but the other two are 2·5 Å. Reference was made earlier to the importance of the *y* coordinate of the Mg_1 atom. It may be seen from Fig. 3 that the long Mg–O distance is largely dependent on only one

Table 3. *Atomic coordinates*

	Mg_1	Mg_2	Si	O_1	O_2	O_3
x	0·000	0·000	0·292	0·118	0·359	0·348
y	0·265	0·087	0·091	0·097	0·259	0·000
z	0·250	0·250	0·07	0·07	0·07	0·32

Table 4. *Interatomic distances* (Å)

Si–O_1	1·61	Mg_1–O_1	2·07	O_1–O_1''	3·15
Si–O_2	1·59	Mg_1–O_2	2·15	O_1–O_2	2·80
Si–O_3	1·63	Mg_1–O_3	2·52	O_1–O_2'	2·96
O_1–O_2	2·64	Mg_2–O_1	2·02	O_1–O_3	3·24
O_1–O_3	2·65	Mg_2–O_1'	2·17	O_3–O_3''	2·91
O_2–O_3	2·63	Mg_2–O_2	2·11	Mg_1–Mg_2	3·08
O_3–O_3'	2·66	O_1–O_1'	3·14	Mg_1–Mg_2'	3·08

parameter, the y coordinate of the Mg_1 atom. Calculations show (Table 2) that increase of the y coordinate from 0·265 to 0·29 gives a significant worsening of the agreement between the observed and calculated structure factors. This change of the coordinate reduces the distance Mg_1–O_3 only from 2·5 to 2·3 Å, still leaving a value greater than the 2·1 Å value for all the other Mg–O distances. Thus it is taken that this distance is genuinely much longer than the other ones around the Mg_1 atom. The long distance goes to the O_3 atom, which is already bonded to two silicon atoms and which, on a strict interpretation of the valence bond rule, should already be satisfied by the bonding to the silicon atoms. Thus it is not surprising to find the Mg_1 atom further away from the O_3 atoms than from the O_1 and O_2 atoms. Nevertheless the coordination is very irregular, especially as the two long distances are adjacent in the Mg_1 polyhedron, and is regarded as the weak point of the structure.

Clino-enstatite, the monoclinic form of $MgSiO_3$, also shows pseudo-symmetry, the true lattice being primitive and the pseudo-lattice *C* face-centered. Although a detailed analysis of the pseudo-symmetry of clino-enstatite must await the completion of the structure refinement by Dr N. Morimoto, it seems safe to say that the pseudo-symmetry arises from a slight collapse and twisting of the silicon–oxygen chains about the relatively small Mg ions. In diopside, the type structure of monoclinic pyroxenes, the Ca ions are sufficiently large to hold the structure in the more symmetrical arrangement. The irregular shape of the Mg_1 polyhedron of proto-enstatite in which the Mg_1–O_3 distances are greater than normal indicates that the pseudo-symmetries of both proto- and clino-enstatite arise from the relative smallness of the Mg ion.

At higher temperatures, where proto-enstatite may be the stable form of $MgSiO_3$, the Mg_2 atom along with other atoms will be vibrating considerably more and should fill the cavity more effectively. Furthermore, the known increase of solid solution with higher temperatures for many compounds shows that structural tolerance for valence mis-balance and size discrepancy is generally greater. For these two reasons, it is thought that the poor coordination of the Mg_1 atom will become of lesser importance at higher temperature, allowing proto-enstatite to become more stable.

The cooperation of Drs F. R. Boyd, N. Morimoto and J. F. Schairer of the Geophysical Laboratory was most valuable. This investigation forms part of a programme of fundamental research on the pyroxenes, supported by the National Science Foundation.

References

Atlas, Leon (1952). *J. Geol. Chicago*, **60**, 125.
Boyd, F. R. & Schairer, J. F. (1957). *Bull. Geol. Soc. Amer.* **68**, 1703 (abstr.).
Foster, W. R. (1951). *J. Amer. Ceram. Soc.* **34**, 255.
Smith, J. V. (1954). *Acta Cryst.* **7**, 479.

Acta Cryst. (1959). **12**, 519

The Crystal Structure of Sr_4PtO_6 and Two Related Compounds*

By John J. Randall, Jr. and Lewis Katz

Department of Chemistry, The University of Connecticut, Storrs, Connecticut, U.S.A.

(*Received* 30 *October* 1958 *and in revised form* 5 *January* 1959)

The crystal structure of Sr_4PtO_6 has been determined by a trial and error method. The crystals are trigonal with space group $R\bar{3}c$; the triply primitive hexagonal cell dimensions are $a = 9{\cdot}74$, $c = 11{\cdot}90$ Å. The platinum ions are octahedrally coordinated with oxygen and are linked in the c direction through strontium ions surrounded by trigonal prisms of oxygens. These strings of coordination polyhedra are connected laterally by strontiums in eight fold coordination with oxygen. This structure is of the same type as that reported for K_4CdCl_6. The isolation of one PtO_6 group from the next is postulated as a reason for the ease of hydrolysis of the compound. Sr_4IrO_6 and Sr_4RhO_6 have the same structure.

Introduction

In the course of an investigation of the interaction of the alkaline earth oxides with platinum metal oxides, we have prepared and studied compounds with the formulas Sr_4PtO_6, Sr_4IrO_6, and Sr_4RhO_6.† Powder photographs indicated that these compounds had essentially the same structure. In contrast to the behavior of most ternary oxides, these compounds

---

* Part of this work was supported by a contract between the Office of Naval Research and The University of Connecticut. Reproduction in whole or in part is permitted for any purpose of the United States Government.

† The compound containing Rh was shown to be oxygen deficient.